Biointerface Research in Applied Chemistry
Open-Access Journal (ISSN: 2069-5837)

Article
Volume 13, Issue 1, 2023, 55
https://doi.org/10.33263/BRIAC131.055

Magnetic Peristaltic Ciliary Flow Regulates an Embryo Growth in the Human Fallopian Tube

Kayalvizhi Joshua [1], Vijaya Kumar Avula Golla [1,*]

[1] Department of Mathematics, SAS, Vellore Institute of Technology, Vellore-632014, India; jkayal.maths@gmail.com (K.J); vijayakumarag@vit.ac.in (V.K.A.G);
* Correspondence: vijayakumarag@vit.ac.in (V.K.A.G);

Scopus Author ID 8227441000
Received: 17.11.2021; Accepted: 17.12.2021; Published: 30.01.2022

Abstract: The flow transport behavior in a peristaltic-ciliary fallopian tube in the human system caused by a sinusoidal pressure gradient due to magnetic lines of force has been investigated. A descriptive prototype model is established and presented in cylindrical coordinates for the fallopian tapered tubal linearly viscous fluid influenced by an external magnetic force in the human body. Under the wavelength approximation, the consequential partial differential equations governing this biological phenomenon are solved analytically. The solutions obtained are presented in modified Bessel functions of zeroth order of the first kind. Also, solutions are obtained for the velocity components along the axial and the radial directions, pressure gradient, pressure differences over a wavelength, and the stream function. The impacts of the various physical quantities of interest on the momentum transport, wavy curve patterns depicting the velocity range, and the pressure change are plotted. A comparison study of peristaltic, peristaltic-ciliary, and magnetic peristaltic-ciliary flows is also presented as a special case. Furthermore, the embryo's development in the interior of the narrow fallopian tube intramural fluid coming from the ampulla is discussed.

Keywords: peristaltic-ciliary flow; fallopian tube; magnetic field; modified Bessel function.

Nomenclature:

A	The metachronal cilia wave of amplitude	Re	Reynolds number
B_0	Magnetic field applied	U,w	Velocity components
b	The sinusoidal wave of amplitude	$d_z p,\beta$	Pressure gradient
F	Sinusoidal wave propagation	t_r	Residue time over the wavelength
G	Metachronal wave propagation	ψ	Stream function
H	Wave traveling scale	Q_T	Time mean volume flow
h	Traveling wave	ε	Metachronal wave parameter
I_0,I_1	Modified Bessel functions zeroth order of first kind	ϕ	Amplitude ratio
K	Constant	λ	Traveling wavelength
m	Magnetic field	μ	Viscosity
q	Volume flow rate	ρ	Density
R,Z	Radial and axial coordinates	$\Delta p\lambda$	Pressure difference over the wavelength

1. Introduction

In the hollow female abdomen, a couple of lengthy muscular, very narrow tubes exist, called fallopian tubes. Geometrically this one appears in the form of a cylinder, with measurements, length-wise 10 cm to 13 cm, with a diameter varying in the range (0.5 cm, 1.2 cm). The fallopian tube has periodic peristaltic shrinkages with an internal mucous membrane layer, which is crammed

with ciliary cells of distinct heights. Each cell has a length in millimeters about 10 to 0.5 and with radii of 5 mm to 0.125 mm [1-10]. Fallopian tubes, also known as uterine tubes or oviducts, are lengthy narrow tubes existing in the human female abdomen cavity that allow sperm cells to the egg from the ovary, providing a perfect environment for fertilization to the central lumen of the uterus. Most fallopian tubes are rarely 3-4 inches in length, about 0.1-0.3 inches in radius.The tube passage is aligned with many folds consisting of a mucous membrane layer, and thereafter, this consists of muscle tissue with three layers; the interior layer has a spiral shape with organized stuff, the mid one is in a circular shape, and the furthest layer with the stuffs of longitudinal which ends in fimbriae, nearer to the ovaries. The major constituents of fallopian narrow tube fluid are glucose, sodium, and chloride, protected by calcium and several proteins supplements and lactic acids. These constituents occur as a combination of bicarbonates and lactic enzymes and play a vital role in the growth of egg fertilization as well as in the oxygen supplement to the sperm. The main nutrient in the growth of eggs and sperm is glucose. At the same time, the other chemicals support a comfortable environment to ensure fertilization.

Studies show that these secretory cells dispense the least amount of fluid through the fallopian tube; this keeps the alive embryo and the ovum to sustain the growth of the embryo in the uterus [11-13]. The periodic peristaltic shrinkages of the surface tube progress as oscillatory waves [14-24]. The wavelets progressing in a sinusoidal pattern are termed fallopian-cilia flow, which is said to be one of the important transportations in the fluid tube to intramural, the extreme regime of the tube. Due to this transportation, the fully developed embryo flows into the uterus of a non-pregnant (further peristaltic contractions), helping the uterus to afford by assisting the embryo's growth in the whole procedure of human reproduction [25-28]. A linearly viscous peristaltic incompressible flow in a channel of fallopian tubal fluid about embryo transport has significant applications, as suggested by Eytan *et al*.- [29]. It also has important uses in the uterine cavity. [30]. Muhammad Mawlood and Malath Sagban abide [31] show that endometriosis affects the peristaltic-ciliary transit of a developing embryo through the fallopian tubal fluid in the human fallopian tube. Biomechanically explains the transplantation of growing embryos into the human fallopian tube [32-38]. Ashraf *et al*. [39] developed a mathematical model on the peristaltic-ciliary flow of a human fallopian tubal fluid and brought out some interesting results. Based on these studies in the literature, we have been motivated and carried out the following research work, which is biologically significant.

To the best knowledge of the author’s, transport phenomena of the peristaltic-ciliary flow of embryo development in the human fallopian narrow tube influenced by the magnetic field have not yet been addressed. Hence, this article aims to investigate the effects of the field of magnetism over transport characteristics. The solutions of the governing problem are obtained analytically, and the numerical results obtained for this investigation are presented with a comparison study with the sources of published results with previous studies. It is noted that the emerging parameters affect the flow significantly. These effects are reported and analyzed with graphical representations and with physical reasoning.

2. Mathematical Description

Based on the physical geometry of the fallopian tube, it is customized to write the governing equations in cylindrical coordinates by choosing the $\bar{Z}$-axis in the flow direction; that is, over the narrow tube and $\bar{R}$ in straight up with the horizon. The motivation is to study the peristaltic-cilia transport that helps the embryo’s growth in the tube of human fallopian fluid. The biological

structure of the human fallopian tube and the narrow tube with axes of coordinates along the tube have been shown in Figure1. The fluid of the embryo is linear, viscous, and incompressible, and the flow is bi-directional with the impact of a magnetic field of strength B_0, applied externally to get the outer control on the system: It has significance in surgical administration of medication. The surface tube is assumed to have the property of peristaltic contractions and lined interactions with the mucous membrane layer. The main pursuit of the phenomena is that the most crowded mucous and membrane with secretory cells have different attitudes in the fallopian tube. The formation of least volume in the fallopian tube due to the secretory cells, whereas the variation of the heights in cilia cells form hair, alike structure. In the fallopian tube, the contraction of peristaltic motion and oscillations of cilia tip throughout the process. This entire phenomenon is modeled as:

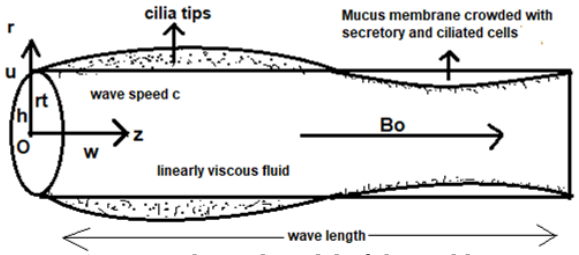

Figure 1. Physical model of the problem

$$\bar{F}(\bar{n})+\bar{G}(\bar{n})=-r_t+\bar{H}(\bar{n}) \tag{2.1}$$

In the above equation, *F(z, t)* describes sinusoidal peristaltic wave propagations for different speeds of amount c, and b is the amplitudes of waves

$$\bar{F}\left(\bar{n}\right)=b\sin\left(\frac{2\pi}{\lambda}\bar{s}\right) \tag{2.2}$$

$$\bar{G}\left(\bar{n}\right)=\sin\left(\frac{2\pi}{\lambda}\bar{s}\right)\cos\left(\frac{2\pi}{\lambda}k\bar{s}\right)Ab\frac{2\pi}{\lambda} \tag{2.3}$$

where $G(z,t)$ describes metachronal wave propagation while $\bar{s}=\bar{Z}-c\bar{t}$. Here $\bar{n}=\bar{Z},\bar{t}$, and all the parameters appearing in those equations are defined in the Nomenclature.

Here, we label the cylindrical system in two frameworks. One is a moving frame reference (r,z) in which we consider the flow-through narrow tube to be time-independent. In contrast, another one, in a framework of laboratory reference which includes time dependence, also defined R is the radial direction. Z is the axial direction in laboratory reference, to study the velocity components U, W respectively and the wave traveling scale H, pressure P with all these quantities the following relations are defined.

$$\left.\begin{aligned}&\bar{r}=\bar{R},\ \bar{Z}-c\bar{t}=\bar{s},\\&\bar{u}\left(\bar{r},\bar{s}\right)=\bar{U}\left(\bar{R},\bar{Z},\bar{t}\right)\ and\ \bar{w}\left(\bar{r},\bar{s}\right)=\bar{W}\left(\bar{R},\bar{Z},\bar{t}\right)-c\\&\bar{p}\left(\bar{s}\right)=\bar{P}\left(\bar{n}\right)\ and\ \bar{h}\left(\bar{s}\right)=\bar{H}\left(\bar{n}\right),\end{aligned}\right\} \tag{2.4}$$

Parameters defined for the purpose of the non-dimensionalization of the above equations are as follows:

$$\bar{r}=r\,r_t,\ \ \bar{z}=2\pi\lambda z,\ \ \bar{u}=2\pi cr_t u/\lambda,\ \bar{w}=wc,\ \ \bar{p}=\mu\lambda cp/2\pi r^2 t,\ \bar{h}=h\,r_t$$

The basic equation of cylindrical co-ordinates:

$$r^{-1}\partial_r\left(rv_r\right)+r^{-1}\partial_\theta\left(v_\theta\right)+\partial_z\left(v_z\right)=0 \tag{2.5}$$

$$\rho\left(\partial_t(v_r)+v_r\partial_r(v_r)+v_\theta r^{-1}\partial_\theta(v_r)+v_z\partial_z(v_z)\right)=\rho g_r-\partial_r p+\mu\left(r^{-1}\partial_r\left(r\partial_r(v_r)\right)+r^{-2}\partial_\theta^{\,2}(v_r)-2r^{-2}\partial_\theta(v_\theta)-v_r r^{-2}\right) \tag{2.6}$$

$$\rho\left(\partial_t(v_z)+v_r\,\partial_r(v_z)+v_\theta r^{-1}\,\partial_\theta(v_r)+v_z\,\partial_z(v_z)\right)=\rho g_z-\partial_z p+\mu\left(r^{-1}\,\partial_r\left(r\,\partial_r(v_z)\right)+r^{-2}\,\partial^2_\theta(v_z)+\partial^2_z(v_z)\right) \quad (2.7)$$

The governing flow of 2D viscous incompressible, varying linearly with negligible thermal effects and body force in the moving reference frame are given in non-dimensional form as follows:

$$r\partial_r u+u+r\partial_z w=0 \quad (2.8)$$

$$(Re)\alpha^3\left(u\partial_r+w\partial_z\right)u=-\partial_r p+\alpha^2\partial_r\left(r^{-1}\partial_r\left(ru\right)\right)+\alpha^4\partial_r{}^2 z \quad (2.9)$$

$$(Re)\alpha\left(u\partial_r+w\partial_z\right)w=-\partial_z p+\frac{1}{r}\partial_r\left(r\,\partial_r\right)w+\alpha^2\partial_z^2 w-\sigma B_0{}^2\left(\overline{w}+c\right) \quad (2.10)$$

where $\alpha=\frac{2\pi r_t}{\lambda}$ is the wave-number, while the notations ∂_r, ∂_z and ∂_θ used to represent the

Partials of the variables r, z, and θ respectively, Reynolds number $(Re)=\frac{cr_t}{\gamma}$. With the utility of the transformation given by the Eq. (2.4) and non-dimensional scaling parameters, the traveling wave Eq. (2.1) implies that

$$h(z)=\varepsilon\varphi\cos(kz)\sin z+\varphi\sin z+1 \quad (2.11)$$

In which amplitude quotient $(\varphi)=\frac{b}{r_t}$, metachronal wave propagation $\not\in=\frac{2\pi A}{\lambda}$.

In moving of the dimensionless form of Eq.(2.4) is given by the Eq.(2.11) along with associated conditions defined at boundaries given by Eq.(2.9) -(2.10) as follows:

$$u(r,z)=0,\quad \text{at } r=0 \qquad u(r,z)=-\frac{dh}{dz} \quad \text{at } r=h \quad (2.12)$$

$$\partial_r w(r,z)=0,\quad \text{at } r=0 \quad w(r,z)=-1 \quad \text{at } r=h \quad (2.13)$$

It is assumed that Re is an order of 10^{-3}, hence the wavelength λ is very large in comparison to the tube radius (r_t), it is observed from the references [9,16,17]. Under these assumptions, Eq. (2.9) and Eq. (2.10) reduce to

$$\frac{dp}{dr}=0 \quad (2.14)$$

$$\frac{dp}{dz}=\frac{1}{r}\frac{\partial}{\partial r}\left(r\frac{\partial w}{\partial r}\right) \quad (2.15)$$

From Eq. (2.14), it is evidence that p is a function of z alone. Thereafter, Eq. (2.14) reduces to

$$r\frac{\partial^2 w}{\partial r^2}+\frac{\partial w}{\partial r}=r\frac{dp}{dz} \quad (2.16)$$

Eq. (2.16) represents the Bessel differential equation of second order, by solving analytically subject to the boundary conditions given in Eq. (2.13), one acquires

$$w(r,z)=\frac{d_z p}{m^2}\left[\frac{I_0(mr)-I_0(mh)}{I_0(mh)}\right]-1 \quad (2.17)$$

is the solution for velocity in the z-direction of the ciliary flow.

The corresponding time residue on wavelength, tr, is:

$$t_r=\int_0^{2\pi}\frac{1}{w(r,z)}dz \quad (2.18)$$

during the integration process, it is treated that r is constant and $\bar{t} = t_r \lambda / 2\pi$, t_r is computed with the substitution of Eq.(2.17) in the Eq.(2.18). And with the use of conditions given by the Eq.(2.12), the radial velocity and pressure gradient of the ciliary flow are derived as follows:

$$u(r,z) = \frac{d_z{}^2 p}{m^2}\left[\frac{r}{2} - \frac{I_1(mr)}{I_0(mh)}\right] \tag{2.19}$$

$$\frac{dp}{dz} = \frac{-2m^2 I_0(mh)}{hI_0(mh) - 2I_1(mr)} h(z) + D \tag{2.20}$$

in which D, is the integral constant to be found. Using $\frac{dp(0)}{dz} = -\beta$ (β is arbitrary fixed value defined at tube entrance of the pressure gradient) into Eq. (2.17), it is computed as

$$\frac{dp}{dz} = \frac{2m^2 I_0(mh)}{hI_0(mh) - 2I_1(mr)}\left[1 - h(z)\right] - \beta \tag{2.21}$$

is the solution for the gradient of pressure nearer to the tube passage of the ciliary flow. The pressure difference over wavelength $\Delta p\lambda$ in a dimensionless form is defined as

$$\Delta p\lambda = \int_0^{2\pi} \frac{dp}{dz} dz \tag{2.22}$$

Then, using Eq. (2.22), it is also computed that pressure difference $\Delta p\lambda$ over the wavelength along with the stream function from Eq. (2.23) and Eq. (2.24) defined as follows:

$$u(r,z) = -r^{-1}\frac{\partial \psi}{\partial z} \tag{2.23}$$

$$w(r,z) = r^{-1}\frac{\partial \psi}{\partial r} \tag{2.24}$$

Then Eq. (2.20) implies that

$$\psi(r,z) = -\frac{r}{m^2}\left[\frac{r}{2} - \frac{I_1(mr)}{I_0(mh)}\right]\frac{dp}{dz} + c_1(r) \tag{2.25}$$

where $c_1(r)$ is the arbitrary constant, it is computed by convection as at the tube midpoint the streamlines are stationary

$$\psi(r,z) = 0 \qquad \text{at } r=0 \tag{2.26}$$

Once completing the arbitrary values with the above equations, we get

$$\psi(r,z) = -\frac{r}{m^2}\left[\frac{r}{2} - \frac{I_1(mr)}{I_0(mh)}\right]\frac{dp}{dz} \tag{2.27}$$

The volume flow rate is given by the Eq. (2.28) as follows:

$$Q = \int_0^H RWdR \tag{2.28}$$

where $Rr_t = R$, $\bar{Z} = \lambda z / 2\pi$, $\bar{t} = \lambda t / 2\pi c$, $\bar{W} = Wc$, and $\bar{H} = Hr_t$.In Eq.(2.23), during the integration process, it is treated that Z and t to be kept stationary, the coordinates, in the moving and laboratory frame of references the axial velocities as well as traveling waves relations are given by

$$\left.\begin{aligned} &z + ct = Z, \quad r = R, \\ &w(r,z) + 1 = W(R,Z,t), \quad h(z) = H(Z,t) \end{aligned}\right\} \tag{2.29}$$

With Eq. (2.28) into Eq. (2.27), yields

$$Q = q + \frac{h^2}{2} \tag{2.30}$$

where

$$q = \int_0^h w(r,z)rdr \tag{2.31}$$

in which q is computed from Eq. (2.31).

Over a time period, T mean time cubic flow of the rate, which is the traveling wave in a given framework, is as follows

$$TQ_T = \int_0^T QdT \tag{2.32}$$

with Eq. (2.31) with the use of Eqs. (2.29) and Eq. (2.30) produces

$$Q_T = q + \frac{1}{2}\int_0^1 h^2 dz \tag{2.33}$$

Eq. (2.32) from Eq. (2.11) gives that

$$Q_T = q + \left(\frac{1}{2}\right) + \left(\frac{23}{50}\right)\varphi + \left(\frac{7}{50}\right)\varphi^2 + \frac{\varepsilon^2\varphi^2 K_1}{32} + \frac{\varepsilon\varphi^2 K_2}{k(k^2-4)} + \frac{\varepsilon\varphi K_3}{(k^2-1)} \tag{2.34}$$

$$K_1 = 2.18 - \frac{\sin(2(1-k))}{1-k} + \frac{2\sin 2k}{k} - \frac{\sin(2(1+k))}{k+1}$$

where

$K_2 = 0.91k\cos k - (2 - 0.17k^2)\sin k$

$K_3 = 0.54\cos k + 0.84\sin k - 1$

Eq. (2.30) written in the form of stream function followed by

$$q = \int_0^h \frac{\partial \psi}{\partial r} dr \tag{2.35}$$

After employing the boundary conditions in Eq. (2.25) and Eq. (2.26) at $r = h$ implies that

$$q = -\frac{h}{m^2}\frac{dp}{dz}\left[\frac{h}{2} - \frac{I_1(mh)}{I_0(mh)}\right] \tag{2.36}$$

3. Results and Discussions

To analyse the flow model of fallopian tubal fluid, the governing equations are solved analytically and presented exact solutions for axial and radial velocity components; pressure gradient; stream-lines; and time over length, in terms of first and zeroth-order modified Bessel functions of the first and second kinds without loss of any generality on the modeling. To focus on the results as a main theme, it is taken to be an appropriate quantitative value followed by a discussion on each plotting through the observation on plotted curves and contours. The impact of various physical quantities was thoroughly studied from the obtained solution. The volume flow rate, the rate at which pressure changes near the tube entrance, and the pressure differences are computed. The influence of the amplitude parameter, the magnetic parameter, the wavelength parameter, and the metachronal wave quantity are investigated. An inclined cross-section at a particular value of $z = \frac{4\pi}{3}$ is considered, while one horizontal, inclined cross-section at r = 0.3 is done to understand the impact of parameters of interest. In Table 1, it is provided that a summary of results of comparison along the radial axis, also provides a contrast between the peristaltic flow and ciliary flow, which usually occurs at $\in$ = 0.00 and 0.15, respectively. In view of the axial

velocity, the peristaltic flow dominates peristaltic-cilia flow. This table also reveals that the current results are in good comparison with the earlier studies considered by the other authors. The maximum velocity is identified in the axial direction because of swaying momentum relative to those at the tips of ciliary oscillating peristaltic vibrations. The negative sign indicates the backward flow.

In Figure 2, axial velocity versus radial are presented at $z = \frac{4\pi}{3}$. The parabolic curves are obtained nearer tube entrance due to pressure gradient: This is true with the changes in the metachronal parameter, amplitude fraction parameter. Also, these velocities are suppressed with enhancement in r and w. The axial and the radial distributions of the velocity components in peristaltic-ciliary flow are much smaller than those in peristaltic flow. It is defined that the amplitude parameter is the ratio of b and r_t, where b symbolizes amplitude of the wave propagation of the peristaltic shrinkages. It is considered that the tube radius as 1.0, hence it is clear that r_t and b vary proportionately while the mechatronic quantity is the ratio of A with λ, where A is the mechatronic cilia wave and λ is the traveling wavelength. If λ assigned as 2π then undoubtedly as A increases, $\in$ also increases. The maximum velocity almost in all figures occurs at the midway of the tube because of not experiencing the shear stresses at the tube wall and no-slip condition.

Figure 3 provides the changes in the axial transport across the cross-section at the tube frontal (0.3, z). It is interesting to note from this figure the impact of the dp/dz at the tubal entry, the ε and the quotient of amplitude ϕ over the axial transport. From figure 3(a) we see that as metachronal quantity increases, the fluid flow transport in the axial direction increases. For tube length of $2\lambda = 4\pi$ (and for the subdivisions of 8 intervals), the axial velocity diminishes in the interval of beginning and next half of wavelength. Figure 3(d) reveals the u(r, z) distribution of the peristaltic flow ($\in$=0.00) and ciliary flow of the peristaltic case ($\in$=0.15). Maximum deviation occurs in the case of u(r, z) compared to the axial distance. The flow is slow in the case of ciliary flow; however, higher in the second wavelength. Vector contour plots are drawn for a certain range of values of the parameters in Figure 4, to point out the local behavior of the ciliary flow of a viscous varying linearly fluid flow. The impacts of dp/dz at the tube entry β, metachronal biological quantity $\in$ and the quotient of amplitude ϕ: These effects on the tubal fluid are shown in Figure 4. From Figures 4(a) to 4(j), the realistic contrast between peristaltic ciliary and peristaltic flow can be seen. It is perceived that these parameters instigate a backword flow.The complete scenario of streamlines indicates that they divide and reaches close to the bolus and navigates such as wavefront.

The entire patterns of streamlines are plotted with forming boluses through Figure 5 to study the effects of the various flow quantities of interest. We see the floating boluses of fluid in an elliptical shape, and the size of the bolus can be described through the dense patter of the streamlines. At the maximum diameter of the tube, these boluses appear strongly while low at minimum diameter length. The effect of β at the entry of the tube on the size of boluses can be understood through the patterns in Figures 5(a) to 5(d). The bolus magnitude was found to shrink with an increase in the pressure gradient. Among these, Figures 5(e) to 5(i) exhibit the impact of amplitude quotient and the metachronal quantity on trapped boluses. With an increase in these quantities, the bolus size tends to increase. A comparison of the study is performed by plotting streamlines of peristaltic-ciliary with peristaltic fluid flow through Figures 5(i) and 5(j): The bolus

size is slightly larger in the ciliary flow of peristaltic. Surprisingly these boluses appear quite smaller at the tube entry. This is due to peristaltic contractions. Further, it can be stated that along with these peristaltic contractions, when there is a swaying motion at the cilia tips, trapped boluses grow.

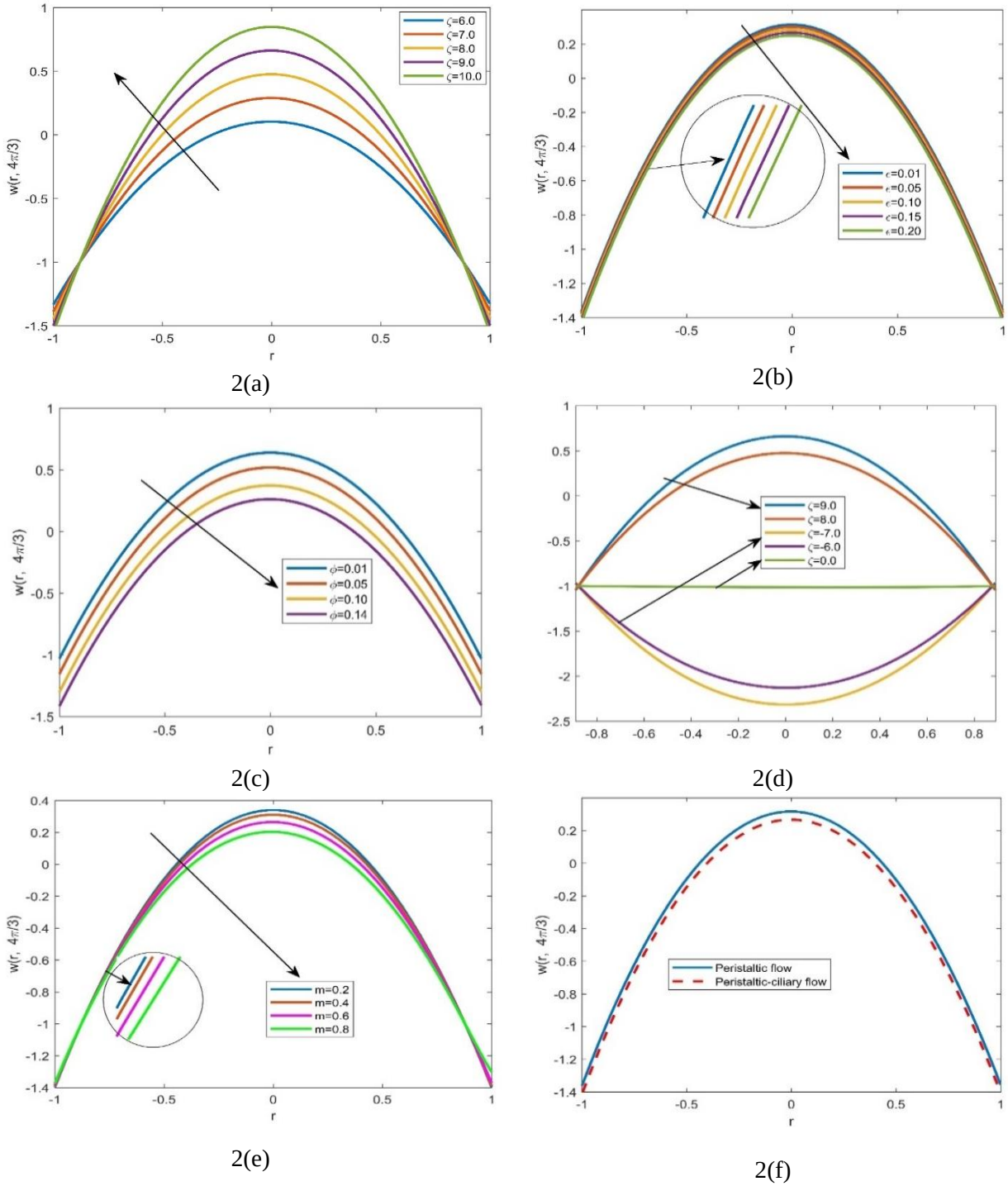

Figure 2. Velocity profiles of Axial velocity against radial distance are plotte when there are variations in 2(a) β (when m=0.1, ε =0.08, ϕ =0.13,and k=1.5), 2(b) ε (when k= 1.5, β = 7.0, ϕ = 0.25and m=0.1),and 2(c) ϕ (when m=0.1, ε = 0.08, k= 1.5and, β =7.0,), 2(d) β (when ε = 0.08 ,m=0.1, k = 1.5,and ϕ = 0.13), 2(e) magnetic parameter , m(ϕ = 0.25, β = 7.0, and k= 1.5) and 2(f) comparative study observing ciliary flow with peristaltic flow (when k= 1.5,, ϕ = 0.19 β = 7.0, and m=0.1) at $(r, 4\pi/3)$.

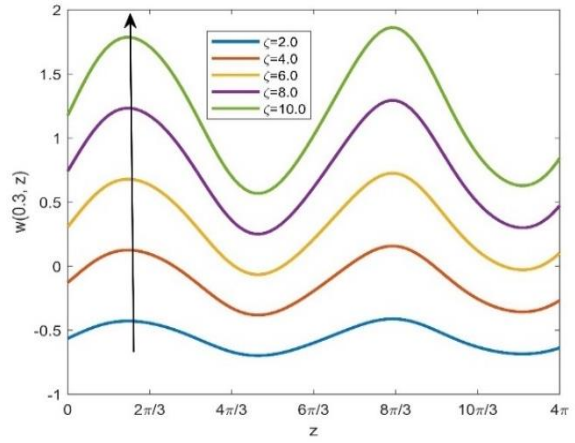

3(a)

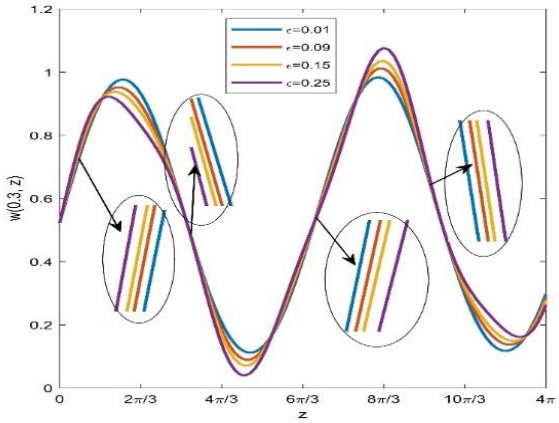

3(b)

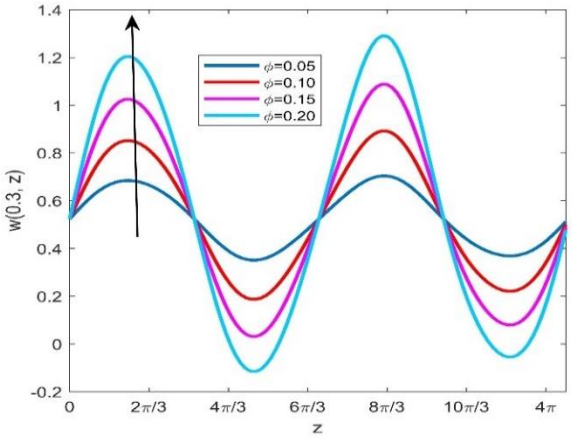

3(c)

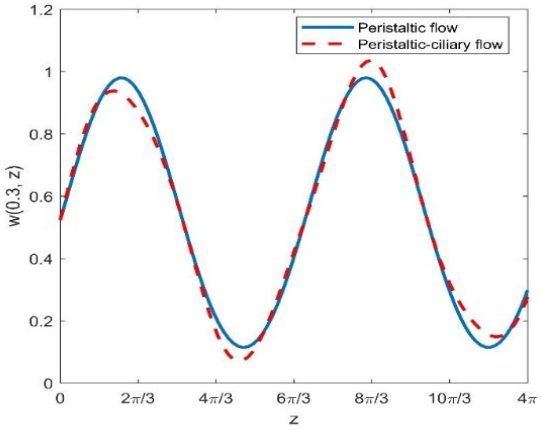

3(d)

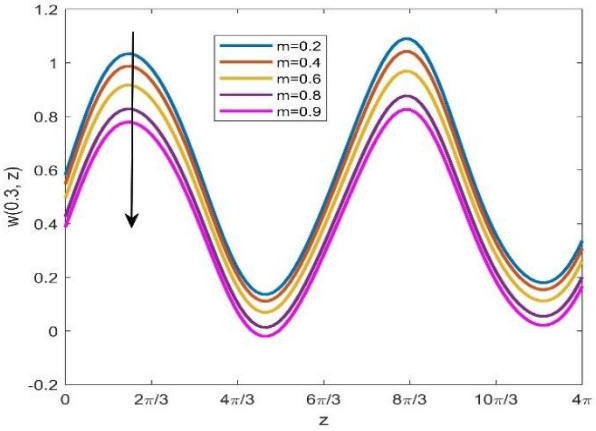

3(e)

Figure 3. Velocity curves for u against z are plotted when there are variations in 3(a) β (when ε = 0.08, m=0.1, k = 1.5,and ϕ = 0.13), 3(b) ε (when ϕ = 0.13, m=0.1, k = 1.5, and β = 7.0),and 3(c) ϕ (when m=0.1, k = 1.5, β = 7.0,and ε = 0.08) 3(d) a comparative study observing ciliary flow with peristaltic flow (when m=0.1, k = 1.5, ϕ = 0.19, and β = 7.0) at (0.3,z) and 3(e) magnetic parameter , m(k= 1.5, β = 7.0, and ϕ = 0.25).

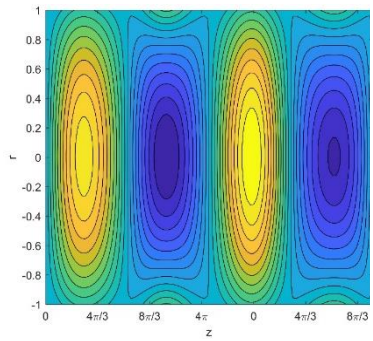

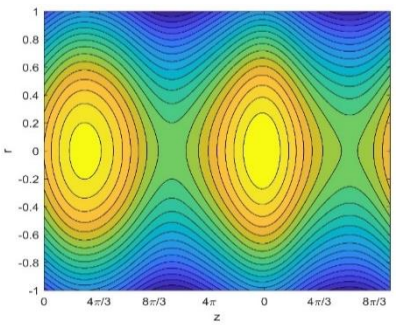

4(b)

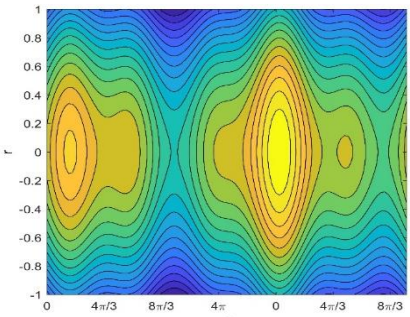

4(c)

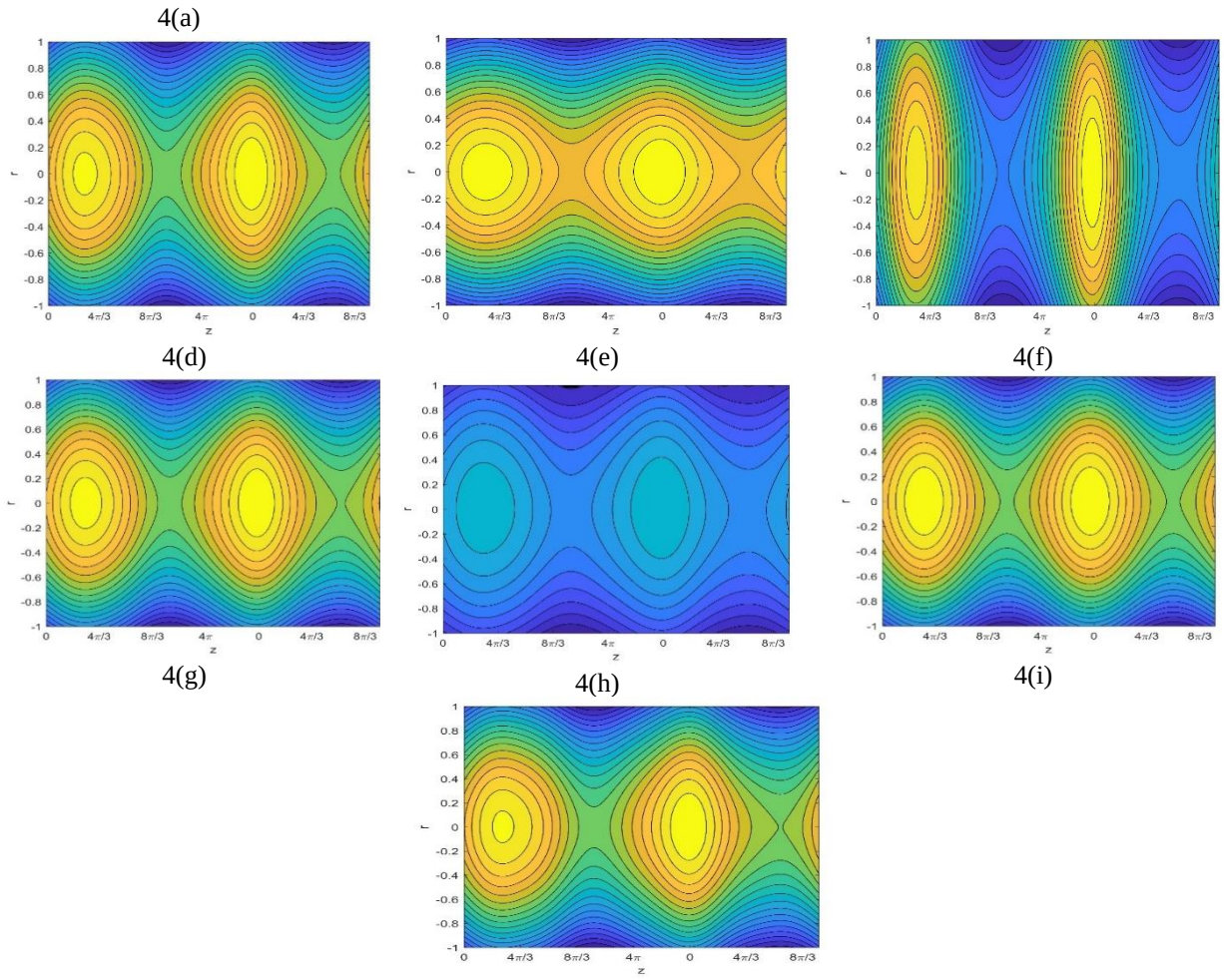

Figure 4. Vector plots of the local flow behavior for various pressure gradients at the tube entrance (4(a) $\beta = 0$, 4(b) $\beta = 1$) when m=0.1, $\varepsilon = 0.08$, k = 1.5, and $\phi = 0.13$, for distinct ε (4(c) $\varepsilon = 0.9$,4(d) $\varepsilon = 0.12$) when m=0.1, k = 1.5, $\phi = 0.13$, and $\beta = 7.0$, and for distinct various ϕ 4(e) $\phi = 0.05$,4 (f) $\phi = 0.6$, 4(g) m= 0.5, and 4(h) m= 0.9 when k = 1.5, $\beta = 10$, $\varepsilon = 0.08$, and a comparative study observing with 4(i) peristaltic flow and 4(j) ciliary flow when m=0.1, $\beta = 10$, $\phi = 0.19$, and k = 1.5.

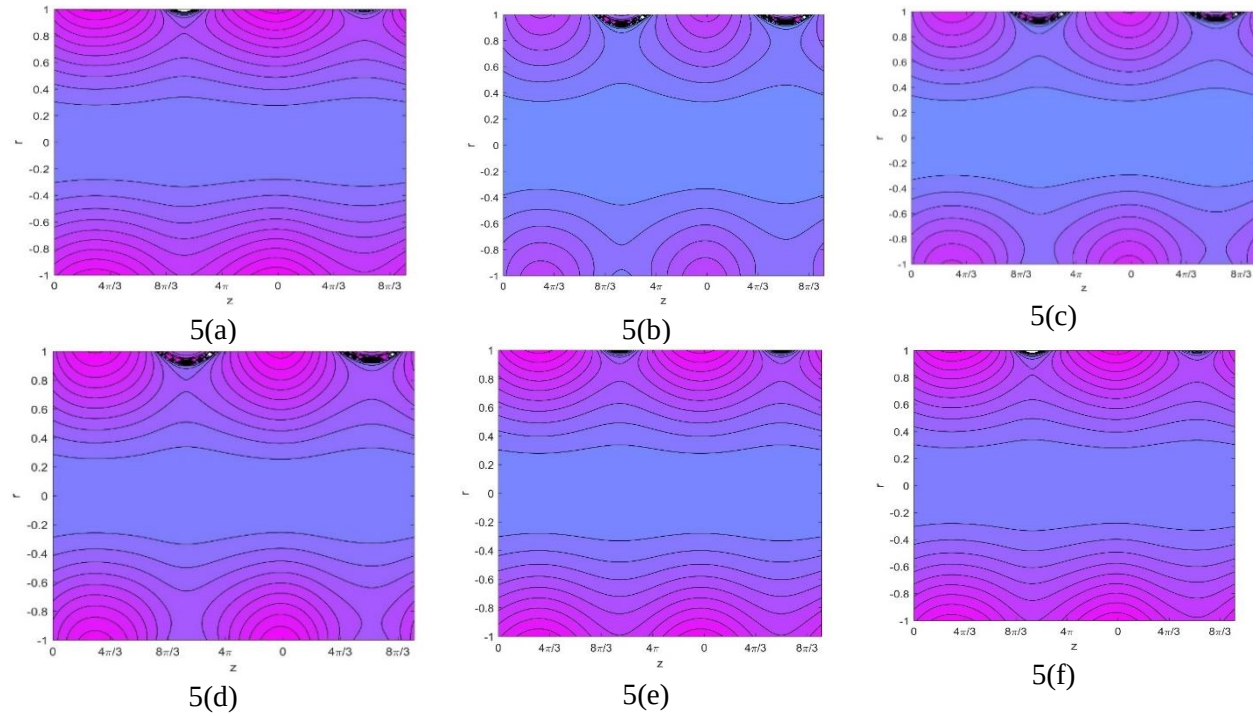

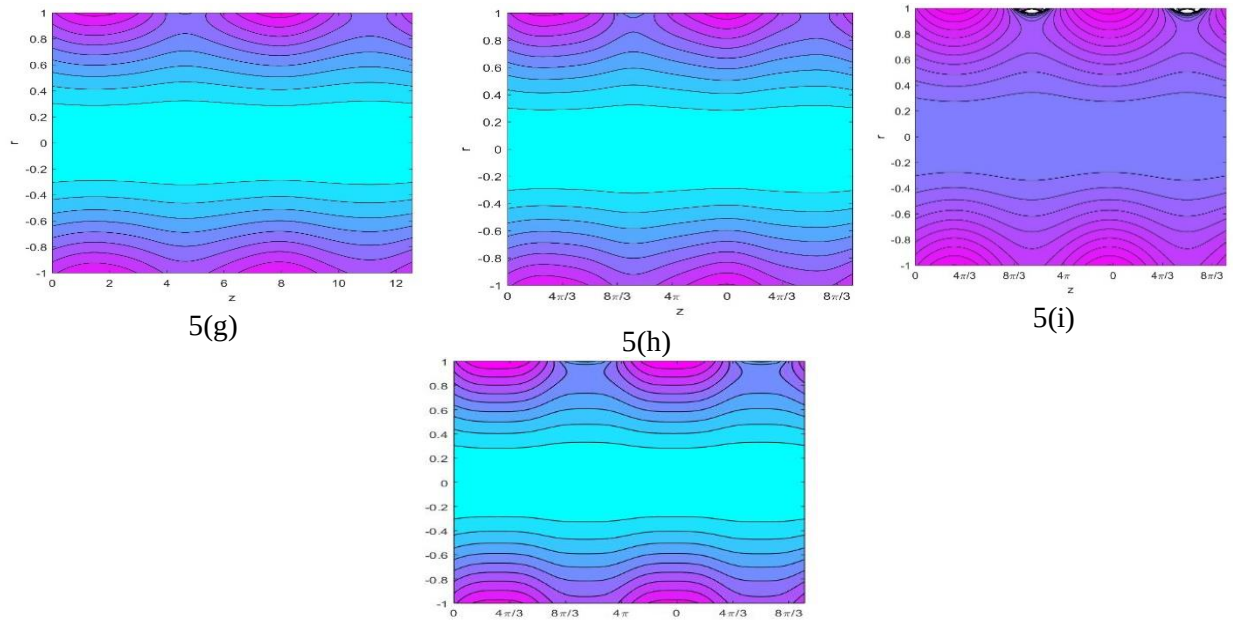

5(g) 5(h) 5(i)

5(j)

Figure 5. stream function plotting with trapped boluses in a dynamic reference frame for variation in the $\frac{dp}{dz}$ at the tube entrance (5(a) $\beta = 9$, 5(b) $\beta = 12$) when m=0.1, $\varepsilon = 0.08$, k = 1.5, and $\phi = 0.13$, for different values of ε (5(c) ε =0, 5(d) =0.08), when m=0.1, $\beta = 8$, $\phi = 0.13$, and k = 1.5, and for variations in amplitude ratio (5(e) ϕ = 0.07, 5(f) $\phi = 0.13$,) when m=0.1, $\varepsilon = 0.08$, $\beta = 8$, and k = 1.5,for variation in magnetic field (5(g)m=0.9,6 (h)m=1) when $\beta = 8$, $\varepsilon = 0.08$, k = 1.5, and $\phi = 0.13$ and comparative study observing with 5(i) peristaltic flow and 5 (j) ciliary flow when m=0.1, $\phi = 0.13$, and k = 1.5.

Table 1. Distribution of the axial velocity along the radial distance when $\varphi = 0.13$, $\xi = 7.0$, $k = 1.5$, $m = 0.1$.

Flow type / r	**Peristaltic flow** $\in$ **=0.00,** $w\left(r, \frac{4\pi}{3}\right)$	**Peristaltic-ciliary flow** $\in$ **=0.15,** $w\left(r, \frac{4\pi}{3}\right)$	**Magnified- peristaltic ciliary flow** $\in$ **=0.15,** $w\left(r, \frac{4\pi}{3}\right)$
	Eytan *et al*. (2001)	**Ashraf *et al*. (2018)**	**Present results**
-1.00	-1.453546	-1.533725	-1.423314781822291
-0.50	0.148408	0.119154	-0.111328082854494
0.00	0.682543	0.670107	0.326162431552843
0.50	0.148408	0.119154	- 0.111328126234323
1.00	-1.453546	-1.533725	-1.423807894397956

4. Conclusions

In a biological context, a theoretical analysis is performed over a human fallopian tubal fluid by considering a linearly varying viscous fluid in a situation of magnetic impact is required during medication. A mathematical model is devolved based on the Navier-Stokes equation in the literature to study the fluid flow phenomena by modeling being done in a cylindrical coordinate system. The model is executed on governing geometrical configuration, which is turned into a Bessel differential equation of non-homogeneous type. The elucidations of results are presented in terms of the first and second kind of modified Bessel function. Consequently, after employing boundary conditions, the Bessel function of the second kind vanishes. And the final solutions involve only the modified Bessel function of the first kind with various orders obtained in the solvation process. The impacts of several physical quantities have been examined, and how the flow field affects and turns to help in revealing the facts as results. In the context of the physics of the problem, exclusively and explicitly presented for axial and radial velocities along with pressure gradient, time residual, and

pressure differences of the considered fallopian tubal fluid. Some of the findings brought out through this investigation are noted as follows. In the radial direction, the axial velocity progresses rapidly at the tube entrance while depressing in a radial direction with an increment in metachronal quantity and amplitude quotient. In the axial direction, this velocity raises in upsurge values of amplitude ratio and near the tube entry point, while it decreases during the beginning wavelength, but during next half wavelength, it results in axial increment. The curves in nature appear in an illustrative fashion nearer to the tube entrance due to the pressure gradient. The model executed on governing geometrical configuration is turned into a Bessel differential equation of non-homogeneous type. The elucidations of results are presented in terms of the first and second kind modified Bessel function. The bolus size is slightly larger at ciliary flow than the peristaltic flow motion. Interestingly these boluses appear quite smaller at the tube. The bolus size is somewhat larger at ciliary flow than at the peristaltic flow. Interestingly these boluses appear quite smaller at the tube entry only because of peristaltic contractions.

Funding

This research received no external funding.

Acknowledgments

The authors would like to thank all the reviewers for their valuable comments and suggestions to improve the quality of the paper.

Conflicts of Interest

The authors declare no conflict of interest.

References

1. Ashraf, H.; Siddiqui, M.A.; Rana, M.A. Fallopian tube analysis of peristaltic-ciliary flow of third grade fluid in a finite narrow tube. *Chinese Journal of Physics* **2018**, *56*, 605-621, https://doi.org/10.1016/j.cjph.2018.02.001.
2. Ashraf, H.; Siddiqui, M.A.; Rana, M.A. Analysis of the peristaltic-ciliary flow of Johnson-segalman fluid induced by peristalsis-cilia of the human fallopian tube. *Mathematical Biosciences* **2018**, *300*, 64-75, https://doi.org/10.1016/j.mbs.2018.03.018.
3. Ali Ahmad, F.; Zahir, S.; Ebraheem, O. Heat transfer analysis of a magneto-bio-fluid transport with variable thermal viscosity through a vertical ciliated channel. *Symmetry* **2019**, *11*, 1240-1260, https://doi.org/10.3390/sym11101240.
4. Eddy, C.A.; Pauerstein, C. Anatomy and physiology of the fallopian tube. *Clinical Obstetrics and Gynecology* **1980**, *23*, 1177-1193, https://doi.org/10.1097/00003081-198012000-00023.
5. Yeung, W.S.B.; Lee, C.K.F.; Xu, J.S. The oviduct and development of the preimplantation embryo.*Reproductive Medicine Review* **2002**, *10*, 21-44, https://doi.org/10.1017/S0962279902000121.
6. Ghazal, S.; Makarov, J.K.; DeJonge, C.J.Egg transport and fertilization. *Global Library of Women's Medicine* **2014**, https://doi.org/10.3843/GLOWM.10317.
7. Fauci, L.J.; Dillon, R. Biofluidmechanics of reproduction. *Annual Review of Fluid Mechanics* **2006**, *38*, 371-394, https://doi.org/10.1146/annurev.fluid.37.061903.175725.
8. Jones, R.E.; Lopez, K.H. *Human Reproductive Biology*, Elsevier: Burlington, **2006**, 253-260.
9. Kolle, S.; Reese, S.; Kummer, W. New aspects of gamete transport, fertilization, and embryonic development in the oviduct gained by means of live cell imaging. *Theriogenology* **2010**, *73*, 786-795, https://doi.org/10.1016/j.theriogenology.2009.11.002.
10. Sokol, E.R. Clinical anatomy of the uterus, fallopian tubes, and ovaries. *Global Library of Women's Medicine* **2011**, https://doi.org/10.3843/GLOWM.10001.
11. Leese, H.J. The formation and function of oviduct fluid. *Journal of Reproduction and Fertility* **1988**, *82*, 843-856, https://doi.org/10.1530/jrf.0.0820843.

12. Leese, H.J.; Tay, J.I.; Reischl, J.; Downing, S.J. Formation of fallopian tubal fluid: role of a neglected epithelium. *Reproduction* **2001**, *121*, 339-346, https://doi.org/10.1530/rep.0.1210339.
13. David, E.; Ariel, J.; Grisaru, D. Biomechanics of Early Life in the Female Reproductive Tract. *Physiology* **2020**, 35, 134-143, https://doi:10.1152/physiol.00028.2019.
14. Buthaud H. *The Influences of Unsymmetry,Wall Slope and Wall Motion on Peristaltic Pumping at Small Reynolds Number*. M. Sc. Dissertation-The Johns Hopkins University Baltimore Maryland **1971,** 9-24.
15. Nadeem, S.; Shahzadi, I. Mathematical analysis for peristaltic flow of two phase nanofluid in a curved channel. *Communications in Theoretical Physics* **2015**, *64*, 547-554, https://doi.org/10.1088/0253-6102/64/5/547.
16. Nadeem, S.; Shahzadi, I. Single wall carbon nanotube (SWCNT) analysis on peristaltic flow in an inclined tube with permeable walls. *International journal of Heat and Mass Transfer* **2016**, *97*, 794-802, https://doi.org/10.1016/j.ijheatmasstransfer.2016.02.060.
17. Nadeem, S; Shahzadi, I. Inspiration of induced magnetic field on nano hyperbolic tangent fluid in a curved channel. *AIP Advances* **2016**, *6*, 015110-015125, https://doi.org/10.1063/1.4940757.
18. Shahzadi, I.; Nadeem, S. Stimulation of metallic nanoparticles under the impact of radial magnetic field through eccentric cylinders: a useful application in biomedicine. *Journal of Molecular Liquids* **2017**, *225*, 365-381, https://doi.org/10.1016/j.molliq.2016.11.062.
19. Shahzadi, I.; Sadaf, H.; Nadeem, S.; Saleem, A. Bio-mathematical analysis for the peristaltic flow of single wall carbon nanotubes under the impact of variable viscosity and wall properties. *Computer Methods and Programs in Biomedicine* **2017**, *139*, 137-147, https://doi.org/10.1016/j.cmpb.2016.10.016.
20. Shahzadi, I.; Nadeem, S. Inclined magnetic field analysis for metallic nanoparticles submerged in blood with convective boundary condition. *Journal of Molecular Liquids* **2017**, *230*, 61-73, https://doi.org/10.1016/j.molliq.2017.01.008.
21. Shahzadi , I.; Nadeem, S. Impinging of metallic nanoparticles along with the slip effects through a porous medium with MHD. *Journal of Brazilian Society of Mechanical Sciences and Engineering* **2017**, *39*, 2535-2560, https://doi.org/10.1007/s40430-017-0727-7.
22. Shahzadi, I.; Nadeem, S. Impact of curvature on the mixed convective peristaltic flow of shear thinning fluid with nanoparticles. *Canadian Journal of Physics* **2016**, *94*, 1319-1330, https://doi.org/10.1139/cjp-2015-0508.
23. Shahzadi, I.; Nadeem, S.; Rabiei, F. Simultaneous effects of single wall carbon nanotube and effective variable viscosity for peristaltic flow through annulus having permeable walls. *Results in Physics* **2017**, *7*, 667-676, https://doi.org/10.1016/j.rinp.2016.12.024.
24. Eytan, O.; Elad, D. Analysis of intra-uterine fluid motion induced by uterine contractions. *Bulletin of Mathematical Biology* **1999**, *61*, 221-236, https://doi.org/10.1006/bulm.1998.0069.
25. Carlson, B.M. *Human Embryology and Developmental Biology*, Elsevier: Philadelphia, **2014,** 36-37.
26. Ezzati, M.; Djahanbakhch, O.;Arian, S.;Carr, B.R. Tubal transport of gametes and embryos: a review of physiology and pathophysiology. *Journal of Assisted Reproduction Genetics* **2014**, *31*, 1337-1347, https://doi.org/10.1007/s10815-014-0309-x.
27. Wakeley, P.W. *Optimisation and Properties of Gamete Transport.* Ph.D. dissertation-University of Birmingham, **2008,** 139-166.
28. Wu, A.; Abbas, S.Z.; Asghar, Z.; Sun, H.; Waqas, M.; Khan, W.A.A shear-rate-dependent flow generated via magnetically controlled metachronal motion of artificial cilia. *Biomechanics and Modeling in Mechanobiology* **2020**, *19*, 1713–1724, https://doi.org/10.1007/s10237-020-01301-y.
29. Eytan, O.; Jaffa, A.J.; Elad, D. Peristaltic flow in a tapered channel: application to embryo transport within the uterine cavity. *Medical Engineering & Physics* **2001**, *23*, 473-482, https://doi.org/10.1016/S1350-4533(01)00078-9.
30. Yaniv, S.; Jaffa, A.J.; Eytan, O.; Elad, D. Simulation of embryo transport in a closed uterine cavity model. *European Journal of Obstetrics&Gynecology Reproductive Biology* **2009**, *144*, 50-60, https://doi.org10.1016/j.ejogrb.2009.02.019.
31. Ahmad mawlood, Dr.; Malathsagban abide. Effect of Endometriosis to fallopian tube of the peristaltic-ciliary flow of third grade fluid in a finite narrow tube. *Journal of Physics:Conference Series* **2020**, *1530*, 012035, https://doi.org/10.1088/1742-6596/1530/1/012035.
32. Farooq, A.A.; Kahshan, M.; Saleem, S.; Mohammad Rahimi-Gorji, ; Fahad S. Al-Mubaddel. Entropy production rate in ciliary induced flows through cylindrical tubules under the consequences of Hall effect. *Journal ofTaiwan Institute of Chemical Engineers* **2021**, *120*, 207-217, https://doi.org/10.1016/j.jtice.2021.03.024.

33. Ashraf, H.; Siddiqui, A.M.; Rana, M.A. Flow analysis of Carreau fluid model induced by the ciliary cells,smooth muscle cells and pressure gradient at the ampullar region entrance. *Theory in Biosciences* **2021**, https://doi.org/10.1007/s12064-021-00352-8.
34. Ashraf, H.; Siddiqui, A.M.; Rana, M.A.; Gawo, G.A. Flow assessment of the shear rate dependent viscoelastic fluid: Application of biomechanics in growing human embryo transport. *Alexandria Engineering Journal* **2021**, *60*, 5921-5934, https://doi.org/10.1016/j.aej.2021.04.055.
35. Wahid Butt, A.; Sher Akbar, N.; Ahmad Mir, N. Heat transfer analysis of peristaltic flow of a Phan-Thien–Tanner fluid model due to metachronal wave of cilia. *Biomechanics and Modeling in Mechanobiology* **2020**, *19, 1925-1933*, https://doi.org/10.1007/s10237-020-01317-4.
36. Maqbool, K.; Manzoor, N.; Ellahi, R.; Sadiq, M. Influence of heat transfer on MHD Carreau fluid flow due to motile cilia in a channel. *Journal of Thermal Analysis and Calorimetry* **2021**, *144*, 2317–2326, https://doi.org/10.1007/s10973-020-10476-6.
37. Nazeer, M; Hussain, F.; Iftikhar, S.; Muhammad, I.K.; Ramesh, K.; Shehzad, N.; Baig, A; Kadry, S.; Chu, Y-M. Mathematical modeling of bio-magnetic fluid bounded within ciliated walls of wavy channel. *Numerical Methods for Partial Differential Equations* **2021,** *37***,** 1-20, https://doi.org/10.1002/num.22763.
38. Alblawi, A.; Sabakeyani, S.; Isakhov, A.; Alarifi Ibrahim, M. Ciliary Flow of Casson Nanofluid with the Influence of MHD having Carbon Nanotubes. *Current Nanoscience* **2021**, *17*, 447-462**,** https://doi.org/10.2174/1573413716999201015090335.
39. Ashraf, H.; Siddiqui, A.M.; Rana, M.A. Fallopian tube assessment of the peristaltic-ciliary flow of a linearly viscous fluid in a finite narrow tube. *Applied Mathematics and Mechanics* **2018**, *39*, 437-454, https://doi.org/10.1007/s10483-018-2305-9.
40. Chumduri, C.; Margherita, Y.; Turc. Organoids of the female reproductive tract. *Journal of Molecular Medicine* **2021**, *99*, 531–553, https://doi.org/10.1007/s00109-020-02028-0.
41. Milana, E.; Zhang, R.; Vetrano, M.R.; Peerlinck, S.; De Volder, M.; Onck, P.R.; Gorissen, B. Metachronal patterns in artificial cilia for low Reynolds number fluid propulsion. *Science Advances* **2020**, *49*, eabd2508, https://doi.org/10.1126/sciadv.abd2508.
42. Zeeshan, A.; Javid, K.; Waqas, M.; Ghaffari, A.; Khan, W.A. Cilia-driven fluid flow in a curved channel: effects of complex wave and porous medium. *Fluid Dynamics Research* **2020**, *52*, 015514, https://doi.org/10.1088/1873-7005/ab67d9.
43. Lyons, R.A.; Saridogan, E.; Djahanbakhch, O. The reproductive significance of human fallopian tube cilia. *Human Reproduction Update* **2006**, *12*, 363-372, https://doi.org/10.1093/humupd/dml012.
44. Maiti, S.; Pandey, S.K. Rheological fluid motion in tube by metachronal waves of cilia. *Applied Mathematics and Mechanics* **2017**, *38*, 393-410, https://doi.org/10.1007/s10483-017-2179-8.
45. Sadaf, H. Bio-fluid fluid flow analysis based on heat transfer and variable viscosity. *Applied Mathematics and Mechanics* **2019,** *40*, 1029–1040, https://doi.org/10.1007/s10483-019-2499-8.
46. Sadaf, H.; Nadeem, S. Influences of slip and Cu-blood nanofluid in a physiological study of cilia. *Computer Methods and Programs in Biomedicine* **2016**, *131*, 169-180, https://doi.org/10.1016/j.cmpb.2016.04.008.
47. Zaher, A.Z.; Moawad, A.M.A.; Mekheimer, Kh. S.; Bhatti, M.M. Residual time of sinusoidal metachronalciliary flow of non-Newtonian fluid through ciliated walls: fertilization and implantation. *Biomechanics and Modeling in Mechanobiology* **2021,** *20*, 609–630, https://doi.org/10.1007/s10237-020-01405-5.
48. Munawar, S.; Saleem, N. Second Law Analysis of Ciliary Pumping Transport in an Inclined Channel Coated with Carreau Fluid under a Magnetic Field. *Coatings* **2020**, *10*, 240, https://doi.org/10.3390/coatings10030240.
49. Sadaf, H.; Nadeem, S. Fluid flow analysis of cilia beating in a curved channel in the presence of magnetic field and heat transfer. *Canadian Journal of Physics* **2020**, *98*, 191-197, https://doi.org/10.1139/cjp-2018-0715.
50. Blake, J.R.; Vann, P.G.; Winet, H.A. Model for ovum transport. *Journal of Theoretical Biol*ogy **1982**, *102*, 145-166, https://doi.org10.1016/0022-5193(83)90267-9.
51. Papanastasiou, T.C. *Applied Fluid Mechanics.* P T R Prentice Hall, Inc., A Paramount Communications Company Englewood Cliffs, New Jersey, **1994**, 309-310.
52. Siddiqui, A.M.; Ashraf, H.; Walait, A.; Haroon, T. On study of horizontal thin film flow of Sisko fluid due to surface tension gradient. *Appied Mathematics and Mechanics* **2015**, *36*, 847-862, https://doi.org/10.1007/s10483-015-1952-9.
53. Ravikumar, R.; Vinodhini, A.F.; Prakash, G. Heat transfer and slip effects on the MHD peristaltic flow of viscous fluid in tapered microvessels:Application of Blood Flow Research. *International Journal of Engineering and Advanced Technology* **2019**, *9*, 5384-5390, https://doi.org10.35940/ijeat.A3073.109119.

54. Hall, J.; Clarke, N. The mechanics of cilium beating: Quantifyingthe relationship btweenmetachronal wavelength and fluid flow rate. *Journal of Fluid Mechanics* **2020**, *891*, A20, https://doi.org/10.1017/jfm.2020.161.